Influence of the exchange-correlation potential in density-functional calculations on polarizabilities and absorption spectra of alkali-metal clusters

S. J. A. van Gisbergen,[1] J. M. Pacheco,[2] and E. J. Baerends[3]
[1]*Scientific Computing & Modelling NV, Section Theoretical Chemistry, Vrije Universiteit, De Boelelaan 1083, 1081 HV, Amsterdam, The Netherlands*
[2]*Departamento de Física da Universidade, P-3004-516 Coimbra, Portugal*
[3]*Section Theoretical Chemistry, Vrije Universiteit, De Boelelaan 1083, 1081 HV, Amsterdam, The Netherlands*
(Received 6 September 2000; published 11 May 2001)

All-electron calculations in large basis sets of excitation energies, oscillator strengths, and polarizabilities of small alkali-metal clusters of Li, Na, and K, with up to eight atoms, are performed using time-dependent density-functional theory. It is shown that the use of the recently developed statistical average of orbital potentials (SAOP) exchange-correlation (xc) potential [P.R.T. Schipper *et al.*, J. Chem. Phys. **112**, 1344 (2000)] leads to polarizabilities of these alkali-metal clusters which are 10–15 % larger than polarizabilities calculated with the xc potential of the local-density approximation (LDA). The lower LDA polarizabilities (in comparison to the SAOP) are shown to originate from differences in the low-lying excitation energies, which are determined by the xc potential in the molecular inner and valence region. In spite of such differences, both SAOP and LDA results are shown to provide reliable assignments of the experimental absorption spectra, with typical errors in peak positions of only 0.1– 0.2 eV, or even less.

DOI: 10.1103/PhysRevA.63.063201 PACS number(s): 36.40.Vz, 31.15.Ew

I. INTRODUCTION

The static and dynamic polarizabilities of alkali-metal clusters (Li_n,Na_n,K_n) have been studied by a variety of theoretical methods (for a recent and complete review, see Ref. [1]), of which configuration interaction (CI) and density-functional theory (DFT) emerge as the most reliable approaches available (see Refs. [2–5] for some recent DFT papers on this topic). At present, no experimental information is available for the equilibrium shapes of atomic clusters, except for the trivial ones. Therefore, as pointed out before [6,7], a comparison between theoretical and experimental results for the polarizability may help us to obtain information on the shapes of such clusters. Moreover, it is of great interest to understand the evolution of the static and dynamical polarizabilities of atomic clusters as a function of size. The interplay between theory and experiment may contribute to a better understanding of the size dependence. Density-functional theory, and its time-dependent extension, time-dependent DFT (TDDFT), provide a useful theoretical framework for studying these properties. The efficiency of this method allows the treatment of the large cluster sizes which are currently accessible experimentally. Furthermore, TDDFT has been shown to provide results of high accuracy in different types of systems, for properties such as excitation energies, oscillator strengths, and polarizabilities. As a result, one may hope to make quantitative interpretations of the experimental results.

The comparison between various TDDFT calculations of optical properties of metal clusters, as well as with experimental data is affected by several factors which preclude an unambiguous comparison. First of all, theoretical calculations typically assume static nuclear positions at zero temperature, which may be a reasonable approximation for certain experiments, but rather far from reality in others. Theoretical studies which go beyond this zero-temperature assumption do exist however [8,9]. Very recently, Kümmel *et al.* [10] calculated how much Na clusters will expand at finite temperatures, and how the polarizabilities of Na_8 and large clusters increase as a result. For smaller clusters temperature effects are expected to be smaller. We will return to these points in more detail.

Second, as stated above, the equilibrium geometries of all but the smallest clusters are generally not known experimentally. The theoretical methods of optimization of cluster geometries face several problems for metallic clusters, such as shallow potential-energy surfaces and, especially for larger clusters, a myriad of local minima. Moreover, different theoretical frameworks do not always agree on the equilibrium geometries as well as on the effective volume of atomic clusters. Clearly, the first and second points are strongly interconnected.

Finally, even if the adopted geometry and the zero-temperature approximation constitute good approximations, other—more technical—issues may further complicate a straightforward comparison between different DFT approaches. We discuss such issues in the following, in connection to the procedures adopted in this work.

In most applications of TDDFT so far, a pseudopotential (PP) approximation has been made to treat the atomic cores. In the present paper, *all* electrons are correlated instead, which is of course preferable in principle. The influence of making a PP approximation is, however, not a subject of the present paper, and is dealt with elsewhere [11].

Another issue which has to be taken into account when comparing different DFT results is the type of basis functions used and the sizes of the basis sets. Popular types of functions used in the study of alkali-metal clusters to date are plane waves [12] (especially in combination with the PP approximation) as well as Gaussian-type orbitals [13,4] (GTO's). More recently, also basis set free PP methods have been applied to alkali metal clusters [14,5]. In this paper,

very large basis sets of Slater-type orbitals (STO's) are used, including many diffuse functions. This approach has been shown to give technically accurate results for various other molecules (see Ref. [15] for an overview of some early applications). Consequently, we expect our results to display only small deviations with respect to basis-set limit and/or basis-set free results.

As is well known, all DFT calculations require approximations to the exchange-correlation (xc) functionals. In the context of TDDFT response theory used for the calculation of the polarizabilities, excitation energies and oscillator strengths, two different xc functionals need to be approximated. The first is the standard static xc potential $v_{\mathrm{xc}}(\mathbf{r})$, which determines the Kohn–Sham (KS) orbitals and orbital energies. These quantities form the starting point for a TDDFT response calculation (for example, the orbital energy differences between occupied and virtual KS orbitals provide a zero-order approximation to the excitation energies). The second approximation is the so-called xc kernel $f_{\mathrm{xc}}(\mathbf{r},\mathbf{r}',\omega)$ which determines the xc contribution to the screening of an externally applied electric field (see below for details). It was found in several papers [16–19] that (i) the xc contribution to the screening provides a (small) correction to the major contribution arising from the Coulomb term; (ii) the adiabatic local-density approximation (ALDA) constitutes a reasonable approximation to $f_{\mathrm{xc}}(\mathbf{r},\mathbf{r}',\omega)$ (we are not aware of xc kernels which have been shown to perform better); and (iii) as a consequence of (i) and (ii), it is more important to improve the approximations to the ordinary xc potential v_{xc} than to the xc kernel f_{xc}. For this reason, we have applied the ALDA for f_{xc} in all calculations presented in this paper.

It should be pointed out that in *exact* DFT, f_{xc} is the functional derivative of v_{xc} which is obtained from E_{xc}. By choosing different types of approximations for the xc potential and the kernel, such relations no longer hold. It would of course be gratifying to have an xc functional which at the same time provides reliable xc energies, and a reliable xc potential and xc kernel. Unfortunately, such a universally reliable xc functional is not yet available and, for the time being, we favor the approach described here.

By carrying out *all* calculations using the same framework, we shall be able to address the main goal of this paper namely, to investigate the role played by the LDA xc potential in the characterization of the electronic properties of metallic clusters, in particular to investigate their dependence on the type of xc potential used. To this end we have selected a few xc potentials which have been developed [20,18], with the specific goal of correcting particular deficiencies inherent to the LDA xc potential. Such potentials are the modified [18] van Leeuwen–Baerends xc potential [20] and the statistical average of orbital potentials (SAOP) xc potential [21,18]. Results obtained with these potentials will be compared with those obtained by more standard LDA potentials such as the parametrization of Vosko, Wilk and Nusair [22].

Small molecules like H_2, H_2O, HF, CO, N_2, and NH_3 have large gaps between the highest occupied molecular orbital (HOMO) and lowest unoccupied molecular orbital (LUMO) and small polarizabilities to which the major contributions come from many high-lying virtuals. For these molecules, the LDA potential leads to overestimated polarizabilities. This trend was confirmed in various papers [23–25] with calculations on roughly 20 different small molecules. The reason for this systematic LDA overestimation is believed to be well understood: because the LDA xc potential is not deep enough in the region of the HOMO orbital and other occupied orbitals which are close in energy, the electrons in these orbitals are too loosely bound and therefore too polarizable.

The alkali-metal clusters studied here form a notable exception to this behavior. Recent *ab initio* studies making use of GTO's [26] have confirmed the picture obtained earlier by means of simplified model calculations [27,28]: that for small sodium clusters, LDA-ALDA polarizabilities are significantly lower (up to 20%) than the experimental ones, measured by Knight *et al.* [29], based on the atomic polarizability values by Molof *et al.* [30]. These alkali-metal clusters therefore question our understanding of the influence of the chosen xc potential on the polarizability. The reason for this different behavior of the alkali-metal clusters is that their polarizabilities are predominantly determined by a few low-lying excitations which carry a large fraction of the total oscillator strength. A reliable description of these low-lying excitations is therefore of crucial importance. The position of Rydberg-like virtuals with respect to the HOMO level is almost irrelevant for these systems. Instead, the position of the LUMO and other low-lying virtuals with respect to the HOMO have to be accurately described. As these orbitals are truly molecular for these systems, and certainly not Rydberg-like, they occupy almost the same region of space as the HOMO orbital, and consequently the polarizability will depend in a subtle way on the form of the xc potential in the (outer) valence region of the molecule.

Dramatic improvements with respect to LDA [18] [both for excitation energies and (hyper)polarizabilities] were recently obtained with the SAOP xc potential, which is given by

$$v_{xc,\sigma}^{\mathrm{SOAP}}(\mathbf{r})=\sum_{i=1}^{N_\sigma} v_{xc,i\sigma}^{\mathrm{mod}}(\mathbf{r})\frac{|\phi_{i\sigma}(\mathbf{r})|^2}{\rho_\sigma(\mathbf{r})}, \tag{1}$$

where σ is a spin label, N_σ is the number of electrons with spin σ, $\phi_{i\sigma}$ is an occupied KS orbital, and ρ_σ is the σ electron density. The individual components $v_{xc,i\sigma}^{\mathrm{mod}}(\mathbf{r})$ are given by an interpolation between two older models for the xc potential:

$$v_{xc,i\sigma}^{\mathrm{mod}}(\mathbf{r})=\exp[-2(\varepsilon_{N\sigma}-\varepsilon_{i\sigma})^2]v_{xc,\sigma}^{\mathrm{LB}\,\alpha}(\mathbf{r}) + (1-\exp[-2(\varepsilon_{N\sigma}-\varepsilon_{i\sigma})^2])v_{xc,\sigma}^{\mathrm{GLLB}}(\mathbf{r}). \tag{2}$$

This form ensures that in the outer region, where the HOMO orbital density $|\phi_{i\sigma}(\mathbf{r})|^2$ is nearly identical to the total density; only the term $i=N_\sigma$ contributes to the sum, and for that term $v_{xc,N\sigma}^{\mathrm{mod}}$ is given by the modified van Leeuwen–Baerends potential $v_{xc,\sigma}^{\mathrm{LB}\,\alpha}(\mathbf{r})$, which is known to be a good approximation in the outer region of the molecule. Similarly, for deeper-lying orbitals, the Gritsenko–van Leeuwen–van Leuthe–Baerends (GLLB) potential [31,32], which contains the atomic step structure required in the inner region, will gain a larger weight. In this way, the SAOP potentials combines the virtues of its constituent parts $v_{xc,\sigma}^{\mathrm{LB}\,\alpha}$ and $v_{xc,\sigma}^{\mathrm{GLLB}}$.

Because of its correct asymptotic behavior and the presence of atomic intershell peaks in the inner molecular region (which are known to be present in the exact xc potential), the SAOP xc potential looks rather different from the LDA xc potential, both in the inner and outer molecular regions. From the performed tests [33,34], it can be concluded that the SAOP potential is reliable beyond the small set of molecules on which it was initially tested, and that it captures certain important aspects of the physics of the xc potential better than LDA or GGA potentials like those of Becke [35] and Perdew [36] (BP). For further details on SAOP we refer to the original paper [18].

We shall compare our LDA and SAOP results to each other, to earlier CI assignments, and to experimental data. This information will be useful for judging the reliability of similar studies on larger clusters and will provide more insight into the nature of the strong (collective) excitations computed and observed in alkali-metal clusters.

The outline of this paper is as follows: after a brief schematic outline of the theoretical methods used, we first compare the average static polarizabilities obtained with the LDA-ALDA, LBα-ALDA, and SAOP-ALDA methods (see below, and Refs. [21,18] for details) at reliable zero-temperature geometries, and compare them to experimental results. The influence of temperature effects will also be discussed. The lower LDA polarizabilities are further analyzed in detail by connecting the results for the polarizabilities to the excitation energies and oscillator strengths.

We proceed with a discussion and analysis of the polarizabilities of larger Li and Na clusters (Li_4, Li_8, Na_4, and Na_8), which will be compared with previous theoretical and experimental results. Finally, we give our conclusions and some prospects for future work.

II. DESCRIPTION OF THE METHOD USED

The TDDFT module of the Amsterdam density-functional program (ADF [37–40]) is used for all reported calculations. This module allows one to calculate, among other things (frequency-dependent) polarizabilities, excitation energies, and oscillator strengths of molecules. The excitation energies and oscillator strengths are obtained from the poles of the polarizability tensor using the method described by Casida and co-workers [41,42]. The frequency-dependent polarizability can be calculated from the first-order change in the electron density when a (frequency-dependent) electric field is applied. In TDDFT theory this first-order density change $\delta\rho(\mathbf{r},\omega)$ can be written as

$$\delta\rho(\mathbf{r},\omega)=\int d^3r'\,\chi_s(\mathbf{r},\mathbf{r}',\omega)v_s^{(1)}(\mathbf{r}',\omega), \tag{3}$$

where χ_s is the KS response function obtained from the (real) KS orbitals and orbital energies:

$$\chi_s(\mathbf{r},\mathbf{r}',\omega)=\sum_i^{\text{occ}}\sum_m^{\text{virt}} n_i\phi_i(\mathbf{r})\phi_m(\mathbf{r})\phi_m(\mathbf{r}')\phi_i(\mathbf{r}') \times\left(\frac{1}{(\varepsilon_i-\varepsilon_m)+\omega}+\frac{1}{(\varepsilon_i-\varepsilon_m)-\omega}\right). \tag{4}$$

$\varepsilon_i(\varepsilon_m)$ are the orbital energies of the occupied (virtual) KS orbitals $\phi_i(\mathbf{r})$ $(\phi_m(\mathbf{r}))$ and n_i is the occupation number of occupied orbital i. The potential $v_s^{(1)}(\mathbf{r}',\omega)$ is the first-order change in the KS potential, obtained as a functional derivative of the KS potential, in which the applied electric field $v_{\text{ext}}(\mathbf{r})$ constitutes the leading term:

$$v_s^{(1)}(\mathbf{r},\omega)=v_{\text{ext}}(\mathbf{r},\omega)+\int d\mathbf{r}'\frac{\delta\rho(\mathbf{r},\omega)}{|\mathbf{r}-\mathbf{r}'|}+\delta v_{\text{xc}}[\,\delta\rho](\mathbf{r},\omega). \tag{5}$$

As a result, the first-order change in the KS potential also contains Hartree (H) and xc screening terms resulting from the corresponding terms above, which are required in the KS picture of noninteracting particles to obtain the correct density change of the interacting electrons. Since the screening terms in the potential $v_s^{(1)}(\mathbf{r}')$ depend upon the density change one is interested in, Eq. (3) is an integral equation for $\delta\rho(\mathbf{r},\omega)$, which is solved in a self-consistent manner in our implementation.

The xc term in $v_s^{(1)}(\mathbf{r}')$ can be written in terms of the xc kernel $f_{\text{xc}}(\mathbf{r},\mathbf{r}',\omega)$ (the Fourier transform of the functional derivative of the time-dependent xc potential with respect to the time-dependent density):

$$\delta v_{\text{xc}}(\mathbf{r},\omega)=\int d\mathbf{r}'\,f_{\text{xc}}(\mathbf{r},\mathbf{r}';\omega)\,\delta\rho(\mathbf{r}',\omega). \tag{6}$$

This kernel needs to be approximated, in addition to the approximation to the xc potential $v_{\text{xc}}(\mathbf{r})$ which is always necessary in DFT.

In previous papers [16–18] it was shown that, for nonmetallic atoms and small molecules, it is of crucial importance to make a good approximation to $v_{\text{xc}}(\mathbf{r})$, while even the simple adiabatic local density approximation for f_{xc} is quite reasonable. In other words, it is important to have a reliable description of the KS response function $\chi_s(\mathbf{r},\mathbf{r}',\omega)$, as determined by the KS orbitals, and the zero-order estimate of the excitation energies given by the KS orbital energy differences $\varepsilon_a-\varepsilon_i$. These conclusions rely upon the fact that, for small molecules of nonmetallic elements, the xc contribution to the screening of the external field is usually not large. Whether this feature applies to alkali-metal clusters at all sizes remains an open question (see, in this context, the discussion in Ref. [43] concerning the self-polarization problem). At any rate, we shall not attempt at improving on the description of $f_{\text{xc}}^{\text{ALDA}}$, using the ALDA throughout, as in previous works, combining it with xc potentials of increasing levels of refinement. As a starting point, the usual LDA xc potential is used, for which we employ the Vosko-Wilk-Nusair [22] parametrization. In order to investigate the influence of a corrected asymptotic behavior of the KS potential on the results, we use a modification of the van Leeuwen–Baerends (LB94) potential [20], called the LBα xc potential [18]. Finally, we use the recently developed SAOP potential, which has been applied with considerable success to some small test molecules [18]. Since the SAOP potential includes modifications of the LDA potential not only on the

TABLE I. Average static dipole polarizabilities (in a.u.) of some small alkali-metal clusters. Comparison of results obtained with various xc potentials (in combination with f_{xc}^{ALDA}) to (estimates of) *ab initio* and experimental results.

Molecule	Expt.	CI	Other *ab initio*	LDA	SAOP	LBα	BP
Li_2	221±4% [45], 229 [58]		209.0 [59]	203.7	223.9	194.1	196.9
Li_4	332±10% [45]	(364)[a]		375.2	413.1, (441)[a]	364.1	365.6
Li_8	561±10% [45]	(660)		578.7	636.7	574.2	571.4
Na_2	270±4% [45], 252[b], 256[c]		256.6 [59]	232.6	265.6	193.8	238.0
Na_4	567±10% [45], 539[b], 546[c]	(552)		490.2	553.6, (588)[d]	447.9	506.8
Na_8	907±10% [45], 869[b]	(860)		748.8 (830)[d]	852.9 (934)[d]	681.1[e]	766.4
K_2	486.5 [60]		462.6[59]	436.3	468.6	353.3	451.3
N_2	11.74			12.27	11.82	11.43	
CO	13.08			13.70	13.02	12.63	

[a]Polarizability obtained in the geometry of Ref. [54] used in the CI calculation.
[b]Experimental values from Refs. [29,30] cited in Ref. [4].
[c]Experimental values from Refs. [29,30] cited in Ref. [26].
[d]Polarizability obtained in the geometry of Ref. [49] used in the CI calculation.
[e]The LB94 average polarizability is 659 a.u.

asymptotic behavior but also in the inner region of the potential, we shall be able to assess the relative importance of each correction to the LDA.

The average molecular polarizability α_{av} is related to the vertical singlet excitation energies ω_i of the system and the corresponding oscillator strengths f_i by

$$\alpha_{av}(\omega)=\sum_i \frac{f_i}{\omega_i^2-\omega^2}. \tag{7}$$

We use this equation to analyze the differences between the LDA, SAOP, and CI results, by making the connection to the absorption spectra, determined by the values for $\{f_i\}$ and $\{\omega_i\}$. Especially if only a limited number of low-lying excitation energies carry most of the total oscillator strength (in a complete basis set the oscillator strengths satisfy the sum rule $\Sigma_i f_i = N_e$, where N_e is the number of active electrons), such an analysis can provide further insights. This is the case for the molecules studied here.

Basis sets

Extensive test calculations were carried out in order to study basis-set effects. A detailed account of those tests, together with a comparison with other approximate methods, such as the PP approximation, was carried out in Ref. [11], to which we refer the reader for details. As a result, we selected the following very large STO basis sets (to which the fit sets were adapted accordingly) for the calculations on all molecules studied here.

For Li (Na) clusters we augmented the largest standard ADF all-electron triple zeta basis set with two polarization functions (standard ADF basis V) by adding a large amount of diffuse functions ($2s$, $3p$, $1d$, and $1f$ basis functions for Li, $2s$, $3p$, $2d$, and $1f$ basis functions for Na). The sizes of the basis sets place our results close to the basis-set limit. Linear dependency problems can occur if so many diffuse functions are added. Only for Na_8 were such problems detected, and 51 linear combinations of atomic orbitals were removed to solve this.

For K, we started from a quadruple zeta basis set (larger than basis V), to which we added $2s$, $3p$, $2d$, and $1f$ diffuse basis functions. These basis sets are therefore much larger than the basis sets used, for example, in Ref. [26], in which good results were obtained already with only one diffuse p function. Further tests with large even-tempered basis and fit sets confirmed the results and conclusions presented in this work, as well as the special importance of including diffuse *p* functions [26]. With these large basis sets we believe to obtain results close to the basis set limit and estimate the effect of further improvements to be smaller than 1% for the polarizabilities.

Typically, further basis-set improvements will lead to slight increases in the polarizabilities. For most of the low-lying excitation energies, we estimate that our results are technically accurate up to 0.01 or 0.02 eV. The errors in higher-lying LDA excitation energies will be a bit larger. The oscillator strengths are somewhat harder to converge, and may vary more than the excitation energies when comparing different basis sets. When differences between basis sets occur, the oscillator strengths usually shift to energetically close-lying excitations. This means that the integrated oscillator strength for a certain energy region will be more stable than the individual oscillator strengths associated with single peaks. Of course, the static polarizability being itself an integrated quantity, it is much less sensitive to the basis-set effect than the oscillator strengths. At any rate, oscillator strengths should be reliable up to typically 5–10 % or better.

III. RESULTS AND DISCUSSION

A. Comparison of average polarizabilities for all clusters with different xc potentials

In Table I, we compare our results with different xc po-

tentials to experimental results and accurate *ab initio* results from the literature, as well as to our estimates based on CI results on absorption spectra from the literature (see below for details). On the bottom two lines the average polarizabilities of N_2 and CO from Ref. [18] are presented, in order to show what we consider to be typical for nonmetallic small molecules. Those average polarizabilities are comparatively small (even with respect to Li_2), and the LDA value is a bit too large in comparison with experiment. The LBα potential lowers the LDA values because of its asymptotic behavior, but it overcorrects somewhat. The SAOP potential, on the other hand, leads to rather good agreement with experiment for N_2 and CO. It is clear that the situation is rather different for the alkali-metal dimers, where the experimental polarizabilities are much larger and underestimated by the LDA. For these molecules, the LBα potential gives even lower polarizabilities than the LDA, which are therefore much too low. The BP polarizabilities in the table are a bit lower than the LDA values for the Li clusters and a bit larger for the Na clusters, but the differences with respect to LDA are small, and the BP potential [or generalized gradient approximation (GGA) potentials in general] therefore share the flaws of the LDA, as could be expected. The SAOP polarizabilities for the diatomics are in much better agreement with the reference values than any of the other xc potentials considered here. For larger clusters the trends remain the same. The SAOP xc potential leads to larger polarizabilities than the LDA, and the LBα potential gives polarizabilities that are too low (even lower than those of the LDA); however, the BP results are close to those of the LDA. In previous studies (such as Ref. [4]) larger effects were reported from the use of GGA potentials instead of the LDA. We attribute this mainly to differences in geometry, and perhaps to a lesser extent also to differences in the approximation for the xc kernel, both of which differences are excluded in the present comparison.

In previous work by one of the authors [44,43], the effect of using a self-interaction-corrected (SIC) LDA potential on the polarizability of Na_8 was considered. A larger polarizability value was found than with the LDA potential itself, which one might be tempted to attribute to the effect of the improved asymptotic behavior of the SIC-LDA potential. However, the present results for the LBα xc potential, and a result from a test calculation with the LB94 xc potential itself, give a *lower* value than the LDA polarizability. This is explained below, where it is shown that the description of the inner region is in fact very important for the polarizability of this molecule. The differences between the LB94 or LBα xc potential and the SIC-LDA xc potential could, therefore be due to subtle differences in the inner region, which is also modified with respect to the LDA potential in both cases.

The zero-temperature approximation inherent in our calculations has some implications that are worth addressing in view of the recent results obtained in Refs. [8,10]. Indeed, based on these calculations, one expects that our zero-temperature results underestimate the average bond lengths of the finite-temperature clusters which are actually investigated experimentally, with corresponding underestimations for the polarizabilities. The deviations with respect to experiments are expected to grow linearly with T [10] as well as with the size of the clusters.

Restricting ourselves to the most recent experimental values, which were recorded at relatively high temperatures ($\sim$1100 K) (those of Ref. [45]), we note that (i) all LDA and SAOP results are too low, and (ii) the underestimation increases with the size of the clusters. These features are indeed consistent with the pictures emerging from Ref. [10]. Since Na_8 was the smallest cluster studied in Ref. [10], only for that molecule can a quantitative correction be attempted. Using the estimate [10] of an 81-a.u. (12 $Å^3$) polarizability underestimation in a zero temperature calculation, we arrive at the corrected values for Na_8 which are given in parentheses in Table I in the SAOP and LDA columns. Both the SAOP and LDA values move closer to the experimental value of 907 a.u., and are within the experimental error bounds. The corrected SAOP result now seems to be a bit high, and the LDA value still a bit low. Unfortunately no estimates of temperature effects are yet available for Li and K clusters, and we will not speculate upon the magnitude of temperature effects for these clusters.

B. Average polarizabilities and excitation energies of Li_2, Na_2, and K_2

In Table II, we collect the experimental results for the excitation energies, oscillator strengths, and average polarizabilities for the dimers Li_2, Na_2, and K_2, as well as our DFT results with various xc potentials at the experimental equilibrium geometries (R_e equals 2.6725 Å for Li_2, 3.0786 Å for Na_2, and 3.923 Å for K_2). Because the experimental geometries are known for the dimers, the temperature can be expected to play a less important role than for the larger clusters, and these systems are probably the most reliable testing ground for the xc functionals.

For Na_2 we find an underestimation of the average polarizability by the LDA, in agreement with Guan *et al.* [26] (they found a larger LDA underestimation due to the use of the LDA geometry instead of the experimental one). Vasiliev *et al.* [5] also found a LDA underestimation with a basis-set free-pseudopotential method, although their value was closer to experiment. The relatively small difference between, on the one hand, the result by Vasiliev *et al.* [5] and, on the other hand, the all-electron results from Guan *et al.* [26] and those from the present work, may well be due to the pseudopotential approximation of Ref. [5], in which only one valence electron per Na atom is treated variationally.

Clearly the LDA polarizabilities for the dimers are too low by about 10%, which sets these molecules apart from the more common ones where the LDA leads to a systematic overestimation. As mentioned above, for molecules with relatively small polarizabilities mainly determined by high-lying excitation energies, the LDA overestimation for the polarizability can be removed by employing an asymptotically correct xc potential, such as the LB94 potential, or its improved and modified variant, the LBα potential used here.

For alkali-metal dimers, the effect of adding the asymptotic LB correction is similar to that for the other molecules: it lowers the polarizabilities, in this case leading to

TABLE II. Lowest dipole-allowed excitation energies and corresponding oscillator strengths using four different xc potentials for alkali dimers at the experimental geometries.

Mol.	Property	Expt.[a] Exc.[b]	LDA/ALDA Exc.[b]	Osc.[c]	SAOP/ALDA Exc.[b]	Osc.[c]	LBα/ALDA Exc.[b]	Osc.[c]	BP/ALDA Exc.[b]	Osc.[c]
Li_2	$1\,^1\Sigma_u^+$	1.74	1.96(+0.22)	0.460	1.98(+0.24)	0.496	1.98(+0.24)	0.456	1.99(+0.25)	0.466
	$1\,^1\Pi_u$	2.53	2.54(+0.01)	0.937	2.46(−0.07)	1.010	2.62(+0.09)	0.962	2.62(+0.09)	0.947
	$2\,^1\Sigma_u^+$	3.78	3.28(−0.50)	<0.001	3.71(−0.08)	0.016	3.45(+0.33)	0.007	3.06(−0.73)	0.005
	$-\varepsilon^{HOMO}/V_{ion}$	5.1127	3.29(−1.82)		4.99(−0.12)		5.32(+0.21)		3.32(−1.79)	
	Sum of osc. str.[d]			1.397		1.522		1.425		1.418
	Contribution to α_{av}[e]			196.1		209.8		189.9		189.2
	Other contr. to α_{av}[f]			7.6		14.1		4.2		7.7
	Total α_{av}[g]	221 [45]		203.7		223.9		194.1		196.9
	S_{-4}[h]			29800		33200		27500		27500
Na_2	$1\,^1\Sigma_u^+$	1.82	2.09(+0.27)	0.627	1.96(+0.14)	0.632	2.24(+0.42)	0.642	2.06(+0.24)	0.628
	$1\,^1\Pi_u$	2.52	2.65(+0.13)	1.061	2.51(−0.01)	1.141	3.00(+0.48)	1.089	2.63(+0.11)	1.049
	$2\,^1\Sigma_u^+$	3.64	3.28(−0.38)	0.012	3.64(+0.00)	0.021	4.06(+0.42)	0.009	3.23(−0.41)	0.009
	$-\varepsilon^{HOMO}/V_{ion}$	4.90±0.01	3.21(−1.69)		4.89(−0.01)		5.48(+0.58)		3.20(−1.70)	
	Sum of osc. str.[d]			1.700		1.794		1.74		1.686
	Contribution to α_{av}[e]			218.2		257.1		185.4		222.4
	Other contr. to α_{av}[f]			14.4		8.5		8.4		15.6
	Total α_{av}[g]	270 [45]		232.6		265.6		193.8		238.0
	S_{-4}[h]			30500		39600		21800		31900
K_2	$1\,^1\Sigma_u^+$	1.45	1.57(+0.12)	0.685	1.51(+0.06)	0.696	1.69(+0.24)	0.685	1.54(+0.09)	0.685
	$1\,^1\Pi_u$	1.91	2.02(+0.11)	1.144	1.98(+0.07)	1.176	2.34(+0.43)	1.161	2.00(+0.09)	1.162
	$2\,^1\Sigma_u^+$	2.85	2.64(−0.21)	0.011	2.76(−0.09)	0.000007	2.98(+0.13)	0.013	2.57(−0.28)	0.004
	$2\,^1\Pi_u$	3.05	2.73(−0.32)	0.011	2.88(−0.17)	0.020	3.07(+0.02)	0.096	2.70(−0.35)	0.010
	$-\varepsilon^{HOMO}/V_{ion}$	4.062	2.686(−1.37)		4.31(+0.25)		4.82(+0.76)		2.67(−1.39)	
	Sum of osc.str.[d]			1.851		1.892		1.955		1.861
	Contr. to α_{av}[e]			414.4		448.6		342.8		430.4
	Other contr. to α_{av}[f]			21.9		20.0		10.5		20.9
	Total α_{av}[g]	486.5		436.3		468.6		353.3		451.3
	S_{-4}[h]			100100		115600		67600		107300
	Av. err. all[i]		0.23(−0.06)		0.09(+0.01)		0.28(+0.28)		0.26(−0.09)	
	Av. err. low lying[j]		0.14(+0.14)		0.10(+0.07)		0.32(+0.32)		0.15(+0.15)	
	Av. err. high lying[k]		0.35(−0.35)		0.09(−0.09)		0.23(+0.23)		0.44(−0.44)	

[a]Reference [61] and http://webbook.nist.gov/

[b]Excitation energies are in eV. In parentheses, we show the deviation with respect to the experimental values.

[c]The oscillator strength in a.u.

[d]Sum of the theoretical oscillator strengths of the three (or four for K_2) excitations given in this table.

[e]Contribution to the average polarizability coming from the excitation energies tabulated here, using $\alpha_{av}=\Sigma_i f_i/\omega_i^2$.

[f]Contribution to the average polarizability coming from all excitation energies not tabulated here.

[g]Total static average dipole polarizability. Sum of numbers under (e) and (f).

[h]S_{-4} determines the low-energy frequency dispersion of the average polarizability $\alpha(\omega)$ according to Eq. (8).

[i]All ten excitation energies in this table.

[j]All six low-lying intense excitation energies in this table; average absolute error and average systematic error.

[k]All four weak, high-lying excitation energies in this table; average absolute error and average systematic error.

even stronger underestimations for the experimental quantities. As is often the case, GGA potentials do not help to solve the LDA problem, as can be seen from the BP [35,36] results in Table I. The reason for this is that the GGA xc potentials are usually not so very different from their LDA counterparts. Finally, the SAOP results in this table are in very good agreement with the experimental values, contrasting with the results with the other xc potentials. We attribute this to the form of the xc SAOP potential, which differs from the LDA xc potential both in the inner and outer regions. Clearly, the description of the inner region seems to play an important role for the alkali-metal dimers.

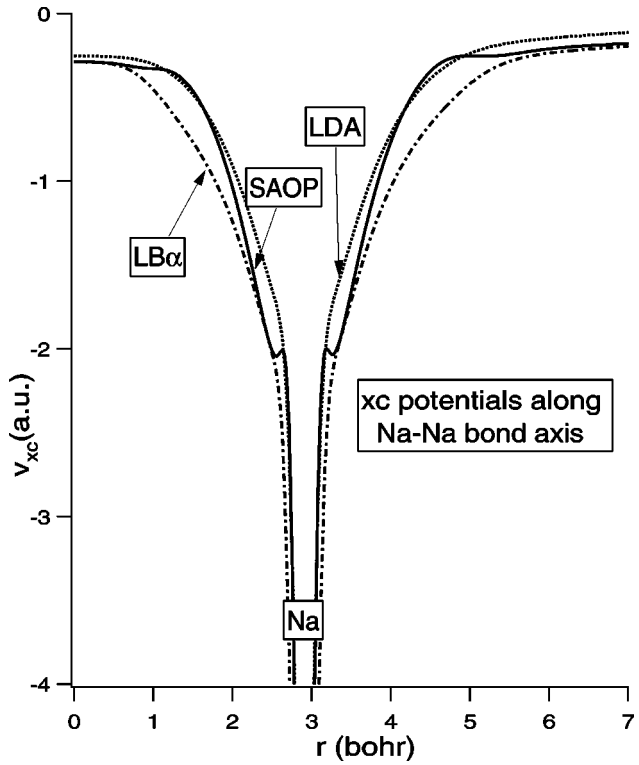

FIG. 1. The LDA, SAOP, and LBα xc potentials for the Na_2 dimer, from the bond midpoint to the outer region.

In order to illustrate the differences in the various xc potentials, they are plotted in Fig. 1 along the Na-Na axis in Na_2, starting from the bond midpoint at $r=0$ to the outer region ($r=7$ bohr). Close to the Na nucleus, the LDA and SAOP potentials nearly coincide, whereas the LBα potential displays a different behavior. In the outer region, the LBα and SAOP potential are very close (in fact, the SAOP was constructed in this way), and tend towards the correct asymptotic Coulombic behavior. In this region, the LDA potential tends to zero too rapidly, and decays faster than the required $-1/r$.

Clearly, in the intermediate, or valence, region, the LBα potential is much deeper (more attractive) than the LDA and SAOP potentials which is consistent with its lower polarizability. A further feature of the SAOP potential consists of pronounced intershell peaks, which also occur in the exact v_{xc}, but which are missing in both LDA and LBα potentials. These peaks strongly affect the potential in the inner valence region, and therefore influence the orbital energies and shape of the occupied and virtual KS orbitals.

In order to understand the behavior of the various xc potentials in more detail, we consider the low-lying dipole-allowed excitations for the dimers and connect the polarizability results to those for the excitation energies and oscillator strengths, using Eq. (7). We also give the values for the HOMO orbital energy $\varepsilon^{\mathrm{HOMO}}$, which should be equal to minus the experimental ionization potential V_{ion} for the exact xc potential. In the case of the asymptotically incorrect LDA and BP xc potentials, $\varepsilon^{\mathrm{HOMO}}$ is much too small in absolute value. As discussed in Ref. [46], this negatively influences the excitation energies which are in this energy range. This is the reason why the LDA and BP excitation energies for the $2\,^1\Sigma_u^+$ for Li_2 and Na_2 and $2\,^1\Pi_u$ for K_2 are clearly underestimated. This problem is solved with the LBα, and especially the SAOP, xc potential.

For the polarizabilities, the description of the $1\,^1\Sigma_u^+$ and $1\,^1\Pi_u$ excitations of L_2, Na_2, and K_2 is of crucial importance, because the corresponding oscillator strengths are large. In fact, the main difference between the alkali-metal dimers and, for example, N_2, can be attributed to the dominant contributions to the polarizability provided by these very low-lying transitions. In N_2, and other more common molecules, the lowest excitation energies lie much higher up in energy (the lowest dipole-allowed excitation energy in N_2 is found near 10 eV), and the contributions to the polarizabilities are spread out over many more excitations. For this reason, the polarizabilities of the alkali metal dimers are also much larger (200–400 a.u.) in comparison to the molecules studied in Ref. [25], which are in the range of 5–40 a.u.

Whereas the contributions from excitations to high-lying virtuals are important for the latter set of molecules, they give only a (relatively) minor contribution to the polarizabilities of the alkali-metal dimers. The contributions of the lowest three or four excitations to the polarizabilities, in the LDA case, amounts to 96%, 93%, and 95% for Li_2, Na_2, and K_2, respectively.

The different values for the polarizabilities can thus be understood from the values obtained for the excitation energies and oscillator strengths of these low-energy transitions. The larger (and improved) polarizability values obtained with the SAOP potential derive from both the larger oscillator strengths and the slightly lower (and better) excitation energies for the most intense transitions.

In fact, the SAOP excitation energies are overall in quite good agreement with experiment, with errors of typically 0.1 eV. This holds for both the high- and low-lying excitation energies, as can be seen from the average errors reported in Table I. The LDA and BP excitations behave quite similarly to each other, are a bit too high for the most intense transitions, and are clearly too low for excitation energies near the HOMO orbital energy.

In Table II, the contributions to the polarizabilities arising from all other, high-lying, excitations are also reported. These contributions are rather small, with a correspondingly small impact on the average polarizability. Therefore, we conclude that it is much more important for these molecules to have a good description of the lowest excitations, for which the description of the (inner) valence region is of crucial importance. The present results for the dimers provide support for the suggestion in Ref. [18] that the SAOP xc potential improves over the LDA in the inner region.

Finally we discuss the Cauchy coefficients S_{-4}, which determine the low-energy frequency dispersion of the average polarizability through the formula

$$\alpha(\omega)=\sum_{k=0}^{\infty} S_{-2k-2}\omega^{2k}, \tag{8}$$

where S_{-2} is the average static polarizability. These coefficients, reported in Table II, follow the same trend as the

TABLE III. Na_4 absorption spectrum in rhombus (D_{2h}) geometry. Comparison of LDA and SAOP results to experimental and CI results.

Label	Expt. [50]		CI [48]			GW-BSE [51]	SAOP			LDA		
	Intens.[a]	Exc. En.[b]	Assign.[c]	Exc. En.[d]	Osc. Str.[d]	Exc. En.[b]	Assign.[c]	Exc. En.[b]	Osc. Str.[d]	Assign.[c]	Exc. En.[b]	Osc. Str.[d]
A	weak	1.63	$1\,^1B_{2u}$	1.51/1.57	0.008/0.002		$1\,^1B_{2u}$	1.64 (+0.01)	0.008	$1\,^1B_{2u}$	1.773 (+0.14)	0.011
B	strong	1.80	$1\,^1B_{3u}$	1.71/1.77	1.18/1.20	2.0	$1\,^1B_{3u}$	1.71 (−0.09)	0.926	$1\,^1B_{3u}$	1.81 (+0.01)	1.067
C	weak	1.98	$2\,^1B_{3u}$	1.87/1.96	0.011/0.016		$2\,^1B_{3u}$	1.87 (−0.11)	0.248	$2\,^1B_{3u}$	2.07 (+0.09)	0.099
D	weak	2.18	$1\,^1B_{1u}$	2.07/2.10	0.075/0.095		$1\,^1B_{1u}$	2.05 (−0.13)	0.097	$1\,^1B_{1u}$	2.24 (+0.06)	0.125
E	strong	2.51	$3\,^1B_{2u}$	2.46/2.63	0.81/0.954	2.65	$2\,^1B_{2u}$	2.47 (−0.04)	1.051	$2\,^1B_{2u}$	2.59 (+0.08)	0.883
E′	weak	2.63	$2\,^1B_{2u}$	2.45/2.57	0.150/0.027		$3\,^1B_{3u}$	2.63 (0.00)	0.023	$3\,^1B_{3u}$	2.70 (+0.07)	0.033
F	strong	2.78	$2\,^1B_{1u}$	2.76/2.90	0.796/0.672	2.95	$2\,^1B_{1u}$	2.78 (0.00)	0.825	$2\,^1B_{1u}$	2.89 (+0.11)	0.231
F′		2.85										
G	weak	3.15	$3\,^1B_{1u}$	3.00/—-	0.083/—		$4\,^1B_{3u}$	3.07 (−0.07)	0.061	$4\,^1B_{3u}$	2.78 (−0.37)	0.001
			$3\,^1B_{3u}$	3.03/—-	0.002/—					$3\,^1B_{1u}$	3.09	0.480
H	weak	3.33	$4\,^1B_{2u}$	3.30/—-	0.056/—		$3\,^1B_{2u}$	3.31 (−0.02)	0.093	$3\,^1B_{2u}$	2.98 (−0.35)	0.163
$-\varepsilon^{HOMO}/V_{ion}$[e]		4.27±0.05						4.31 (+0.04)			2.66 (−1.61)	
Sum osc. str.[f]					3.03 (*A*–*F*)				3.18			2.45
Contr. α_{av}[g]				511.7				514.8			401.1	
Other c. α_{av}[h]				(40)				38.7			89.1	
Total α_{av}[i]		567 [45]		(551.7)				553.6 (588)[j]			490.2	
Av. err. *A*–*F*[k]								0.05			0.08	
Syst. err. *A*–*F*[l]								−0.05			+0.08	

[a]General experimental description of the intensity of the bands.
[b]Vertical excitation energies in eV. In parentheses, we show the deviation from the experimental values.
[c]Assignment of the experimental bands on the basis of their symmetry label. Note that differences occur between CI, SAOP, and LDA results for bands *E*, *E′*, *G*, and *H*.
[d]Oscillator strengths in a.u.
[e]Experimental ionization potential (V_{ion}) and values for minus the orbital energy of the highest occupied molecular orbital (HOMO), which should be identical for the exact xc potential.
[f]Sum of the theoretical oscillator strengths for bands *A*–*F*.
[g]Contributions to average polarizabilities from bands *A*–*F*.
[h]Remaining contributions to polarizability (from higher-lying excitations). The CI number is an estimate based on the SAOP result.
[i]Total average polarizability. Sum of g and h. The CI number is an estimate.
[j]Polarizability obtained in the geometry of Ref. [49].
[k]Average errors in the excitation energies for bands *A*–*F*, according to the assignments given in the table.
[l]Systematic errors in the excitation energies for bands *A*–*F*, obtained by averaging the reported errors without taking absolute values first.

static polarizabilities. The LDA S_{-4} values are lower than the SAOP results and higher than the LBα results for all three dimers. Unfortunately there are no experimental data to compare to for this property.

C. Tetramers Na_4 and Li_4

Unlike the dimers, the experimental geometries for the tetramers Li_4 and Na_4 are not known. However, there seems to be general agreement on at least the shape of the tetramers, which is a rhombus D_{2h} geometry. In this sense the tetramers compare favorably to the octamers, which will be treated below, for which even the shape of the clusters is under debate. Because the shape is determined, we feel there is justification for comparison of our results to theoretical results in the literature and to experimental absorption spectra. Let us now turn to our results for the average polarizabilities, excitation energies, and oscillator strengths for the Na_4 and Li_4 molecules, using the BP-optimized rhombus geometries and the same large basis sets as used for the dimers. The geometries for the tetramers are defined by the lengths of the two diagonals of the rhombus. These are 2.630 and 5.498 Å for Li_4, and 3.107 and 6.358 Å for Na_4. The geometries used in our calculations for the octamers (as well as the tetramers) are available online [47].

1. Polarizability and excitation energies of Na_4

For the polarizability of the Na_4 molecule, reported in Tables I and III, we obtain a value of 553.6 a.u. with the SAOP potential. This is in line with the reported experimental values and with our estimate based on the CI results of Ref. [48]. As for the dimers, the LDA polarizability of 490.2 is too low by about 10%. Although the estimated CI polarizability of 552 a.u. in Tables I and III seems to be in excellent agreement with SAOP and experimental results, it

should be kept in mind that these results were obtained at a different geometry. In fact, if we repeat our SAOP calculation in the geometry of Ref. [49], we obtain a polarizability of 588 a.u., which is 6.2% larger than that obtained at our BP-optimized geometry. If we therefore subtract 6.2% from our estimated CI value, we obtain an average polarizability of 520 a.u., right in between our LDA and SAOP results. It is to be expected that the use of a larger basis in the CI calculations should move this result to somewhat higher values, improving the agreement with the SAOP again.

In order to analyze the Na_4 results in somewhat more detail we turn to the results for the excitation energies and oscillator strengths for Na_4 in Table III. The peaks observed experimentally by Wang *et al.* [50] have been named *A*–*H*. The *B*, *E*, and *F* peaks at 1.80, 2.51, and 2.78 eV are the strongest ones, with the *B* and *E* peaks as the most intense ones. A detailed interpretation of the experimental spectrum was given by Bonačić-Koutecký [48], which we take as our reference data.

First we compare our results to theirs for the lowest energy peaks *A*–*F*, with the focus on the three major peaks *B*, *E*, and *F*. In our discussion we will only talk about the first set of CI results, which are (truncated) all-electron multireference doubles CI (MRDCI) calculations. The second set of CI results come from a MRDCI calculation with an effective core potential (see Ref. [48] for details).

The CI results for the positions of bands *A*–*F* are in perfect agreement with experiment, and the same can be said of both the SAOP-ALDA and LDA-ALDA results. The deviations for bands *B*, *E*, and *F* are, respectively, (-0.09, -0.05, and -0.02) eV for the CI, (-0.08, -0.04, and 0.00) eV for the SAOP result, and ($+0.01$, $+0.09$, $+0.12$) eV for the LDA result. All three methods give the main bands at the experimental positions, with errors of at most 0.1 eV, which is often quoted as a benchmark number for state-of-the-art *ab initio* methods. In fact, these results provide a better description of the experimental data than the computationally more involved *GW* Bethe-Salpeter approach [51], in which the errors are about 0.2 eV for these bands ($+0.20$-, $+0.14$-, and $+0.17$-eV overestimations for bands *B*, *E*, and *F*, respectively). Repeating our SAOP excitation energy calculation at the geometry used in the CI calculation did not lead to large changes, although the excitation energies do shift to slightly lower energies, improving the agreement between the DFT and CI results. We can sum up the Na_4 assignments by stating that both the SAOP and LDA results are in very good agreement with both experimental and CI values, although some differences in assignments remain for the weak G and H bands, for which a more detailed study would be needed.

In order to understand why the LDA polarizability for Na_4 is considerably lower than the SAOP and experimental values, it is useful to have a closer look at the excitation energies and oscillator strengths reported in Table III. In this table, the sum of the oscillator strengths for bands *A*–*F* is given. The SAOP potential finds the largest cumulative oscillator strength in this energy region of 3.18, followed by CI with 3.03 and finally LDA with 2.45 (however, the $3\,^1B_{1u}$ excitation also lies quite low in the LDA, and has a considerable oscillator strength of about 0.5). The dominating contributions of the *A*–*F* bands to the total polarizability clearly show that this low-energy region is very important, and therefore the lower LDA oscillator strength clearly provide a partial explanation of the lower LDA polarizability. Another part of the explanation lies in the excitation energy values. Although the LDA values for bands *A*–*F* are in fact remarkably accurate when compared with results for other molecules, they are systematically above the experimental, CI, and SAOP values. The CI values are always somewhat below the experimental peaks, and the SAOP potential sometimes gives a slightly underestimated, sometimes slightly overestimated value providing, on average, the best agreement with experiment in this case. It has already been mentioned that the experimental peaks were obtained at relatively high temperatures. In a hypothetical $T=0$ experiment, the peaks might shift to slightly higher energies (cf. the Na_n^+ results in Ref. [52]), which would (slightly) worsen the agreement of the CI results with experiment, but improve the agreement of the LDA results. Overall both LDA and SAOP potentials perform well for Na_4.

2. Li_4

The experimental average polarizability value of Ref. [45] is 330 a.u. for Li_4 (see Table I). The LDA value is somewhat higher (370 a.u.), although almost within the experimental error bounds, as is our estimate based on the literature CI results [53] (364 a.u.). The SAOP value is considerably higher (413 a.u.) than the experimental value. The discrepancy between the CI vs. LDA and SAOP results becomes larger if we repeat the DFT calculations at the geometry used in Ref. [54]. Then the SAOP polarizability increases by 7% to 441 a.u. The SAOP excitation energies then shift down by typically 0.03 eV, worsening their agreement with experiment. In what concerns the assignments of the absorption spectra, gathered in Table IV, we find that both the SAOP and LDA results are in very good agreement with the CI assignments, although there are differences in details. The peaks are once again found in very satisfactory agreement with the experimental values with average errors of 0.13 eV for the SAOP potential and an even better 0.08 eV for the LDA potential.

If we consider the sum of the oscillator strengths responsible for the *A*–*E* bands (i.e., the lowest six excitations for CI and the SAOP potential, and the lowest seven for the LDA potential), we find 2.21 for CI, 2.28 for the LDA potential, and 2.55 for the SAOP potential. The overestimated SAOP polarizability can thus be understood from a combination of two factors: a small but systematic underestimation of the excitation energies, and an overestimation of the oscillator strength in this low energy region.

The contributions to the polarizability of these excitations are also listed in Table IV. The LDA and CI numbers are in remarkable agreement and, if we add the contributions from the remaining excitations, also listed in this table, they seem to suggest a polarizability value in the upper half of the experimental error bars. The excellent agreement between the LDA and CI results is partially based on error cancellations: first, the LDA excitation energies are sometimes too low,

TABLE IV. Li_4 absorption spectrum: comparison of TDDFT results (LDA and SAOP) at the BP-optimized geometry vs experimental and CI results of Ref. [53] at optimized geometry.

Label[a]	Exc. En.[b]	Intens.[c]	Assign.[d]	Exc. En.[b]	Osc. Str.[e]	Exc. En.[b]	Osc. Str.[e]	Exc. En.[b]	Osc. Str.[e]
	Expt. [53]			CI [53]		LDA		SAOP	
A	1.801	strong	$1\,^1B_{3u}$	1.78 (−0.02)	0.793	1.68 (−0.12)	0.599	1.66 (−0.14)	0.562
			$1\,^1B_{2u}$	1.81 (+0.01)	0.019	1.69 (−0.11)	0.010	1.64 (−0.16)	0.014
B	2.084	weak	$2\,^1B_{3u}$	2.09 (+0.01)	0.062	2.12 (+0.04)	0.189	2.03 (−0.05)	0.279
C	2.356	weak	$1\,^1B_{1u}$	2.36 (0.00)	0.081	2.16 (−0.20)	0.035	2.05 (−0.31)	0.046
D	2.652	strong	$2\,^1B_{2u}$	2.65 (0.00)	0.681	2.66 (+0.01)	0.775	2.60 (−0.06)	0.870
E	2.928	strong	$2\,^1B_{1u}$	3.01 (+0.08)	0.570	2.92 (−0.01)	0.537	2.85 (−0.08)	0.775
			$3\,^1B_{1u}$			3.07 (+0.14)	0.138	[3.79]	[0.103]
Sum of osc. str.[f]					2.21		2.28		2.55
$-\varepsilon^{HOMO}/V_{ion}$[g]						2.96		4.63	
Contr. to α_{av}[h]				329.3		335.6		380.1	
Other c. to α_{av}[i]				(35)		39.6		33.1	
Total α_{av}[j]	332 [45]			(364)		375.2		413.1 (441)[k]	
Av. err. (eV)[k]				0.02		0.08		0.13	
Sys. err. (eV)[l]				+0.01		−0.06		−0.13	

[a]Experimental label given to bands in Ref. [53].
[b]Vertical excitation energies in eV. Deviations with respect to experiment are given in parentheses.
[c]General description of the experimental intensity of the bands.
[d]Symmetry label for the excitations.
[e]Oscillator strengths in a.u.
[f]Sum of the oscillator strengths for the lowest six (CI, SAOP) or seven (LDA) dipole-allowed excitation energies.
[g]Minus the orbital energy of the highest occupied KS orbital.
[h]Contribution to average polarizability of the lowest six (CI, SAOP) or seven (LDA) dipole-allowed excitation energies, as in the previous tables.
[i]Contribution to the average polarizability from all higher-lying excitation energies, not listed in this table.
[j]Average static dipole polarizability, sum of the terms under h and i.
[k]SAOP polarizability at the geometry of Ref. [54].
[l]Average absolute error with respect to experiment for the excitation energies listed here.
[m]Estimate of the systematic error from the average deviation with respect to experiment without taking absolute values.

sometimes too high; second, the sum of the oscillator strengths is larger in the LDA case, but at the same time it is shifted towards higher energies. Overall the LDA results for Li_4 are very satisfactory.

D. Octamers Na_8 and Li_8

Temperature effects are expected to have a large effect on the octamer results, in particular for Na_8, due to its shallow potential-energy surface. As far as the equilibrium geometries are concerned, the uncertainties are also much larger than for the dimers and tetramers. For the tetramers at least the shape of the clusters is agreed upon. For Na_8 and Li_8 even the symmetry of the clusters is not known with certainty. This should be kept in mind for a comparison to the experimental values below. As regards the comparison to the CI values from the literature, of course we compare to the results obtained for the same symmetry, but that does not fix the cluster shape completely. In the case of Na_8 we reconstructed a geometry with the same symmetry and bond lengths from the literature CI results, in order to check the influence on our results. A synopsis of the results obtained, as well as the CI and experimental results, is provided in Tables V and VI for Na_8 and Li_8, respectively.

1. Na_8

The experimental absorption spectrum [50] of Na_8 is dominated by an intense broad band at 2.5 eV, quite similar to the Li_8 spectrum (see below). Additionally there are much weaker features at 1.68, 2.07, and 2.38 eV. The experimental mean polarizability values range from 870 [29,30,4] (obtained at ≈300 K [55]) to the more recent value of 910 ±90 a.u. [45] (obtained at ≈1100 K). As for the previously discussed sodium cluster results, the differences between the LDA and SAOP results for the absorption spectrum are primarily in the peak positions rather than in their intensities. The LDA peaks are all 0.1 to 0.2 eV higher in energy than the SAOP results. In the CI results, only one *E* excitation carries almost all the oscillator strength. The fact that in a D_{2d} symmetry the principal axes of Na_8 are inequivalent lends support to the fine splitting of the peaks obtained in TDDFT. In spite of this, we have checked whether the difference between CI and TDDFT effects can

TABLE V. Li_8 absorption spectrum: comparison of LDA and SAOP results at BP-optimized D_{2d} geometry to experimental results and CI results at *ab initio* optimized D_{2d} geometry.

Label	Exc. En.[a]	Intens.[b]	Exc. En.[a]	Osc. Str.[c]	Exc. En.[a]	Osc. Str.[c]	Exc. En.[a]	Osc. Str.[c]
	Expt. [d]		CI [e]		LDA		SAOP	
$1\,^1E$			1.07	0.104	0.91	0.028	0.93	0.036
$2\,^1E$			1.48	0.116	1.33	0.053	1.35	0.055
$3\,^1E$			1.70	0.007	1.60	0.011	1.62	0.006
$4\,^1E$	1.82	weak	1.86	0.060	1.83	0.043	1.80	0.044
$5\,^1E$			2.10	0.097	1.93	0.017	1.94	0.018
$6\,^1E$			2.71	0.021	2.67	0.300	2.65	0.492
$7\,^1E$	2.70	strong	2.77	2.970	2.77	1.809	2.72	1.864
$8\,^1E$					2.81	0.007	2.76	0.074
$9\,^1E$					2.83	0.001	2.81	0.011
$10\,^1E$					2.93	0.372	2.91	0.425
$\Sigma_i f_i(E)$[f]				3.375		2.641		3.025
$1\,^1B_2$			1.63	0.001	1.47	0.001	1.46	0.0002
$2\,^1B_2$	1.82	weak	2.01	0.206	1.92	0.153	1.89	0.173
$3\,^1B_2$	2.30	strong	2.56	1.039	2.29	0.139	2.31	0.182
$4\,^1B_2$	2.53	strong	-	-	2.60	1.252	2.56	1.309
$5\,^1B_2$	2.70	strong	-	-	2.96	0.037	2.92	0.035
$\Sigma_i f_i(B_2)$[g]				1.246		1.582		1.699
$-\varepsilon^{\mathrm{HOMO}}$[h]						(3.35)		(5.07)
$\Sigma_i f_i$(total)[i]				4.621		4.223		4.724
Contr. α[j]				581.56		493.0		563.8
Other c. α[k]				(80)		85.7		72.9
Total α[l]		$561 \pm 10\%$		(660)		578.7		636.7

[a]Vertical excitation energies in eV.
[b]General experimental description of the intensity of the bands.
[c]Oscillator strengths in a.u.
[d]Experimental results from Ref. [53].
[e]CI calculations from Ref. [53].
[f]Sum of the oscillator strengths for listed excitations of E symmetry.
[g]Sum of the oscillator strengths for the listed excitations of B_2 symmetry.
[h]Minus the orbital energy of the highest occupied KS orbital (in eV).
[i]Sum of all listed oscillator strengths of both E and of B_2 symmetry.
[j]The cumulative contribution of all listed excitations to the average static polarizability.
[k]Contributions to the average polarizability coming from all higher-lying excitations which are not tabulated here. The CI number is an estimate based on LDA and SAOP numbers.
[l]The total average polarizability (sum of the numbers listed under j and k. The CI number is based on the estimate under k.

be accounted for from differences in the bond lengths between our BP-optimized geometry and the optimized geometry of Ref. [49]. A SAOP calculation at the Na_8 geometry with bond lengths as in Ref. [49], gave results which were much more similar to the SAOP results than to the CI results.

As pointed out in Ref. [8], at higher temperatures (at which the experiments have been carried out) these peaks may merge into the single, broad excitation observed. In keeping with this discussion, the peaks are all located in an energy range of only 0.25 eV and should, therefore, be attributed to the broad intense band at 2.53 eV.

Remarkably, the smaller number of CI excitations carry more cumulated oscillator strength (5.96) than the LDA (5.57) and SAOP (5.84) excitations. This leads to contributions of the listed excitations to the average polarizabilities of 753 (CI), 630 (LDA), and 750 a.u. (SAOP). It is possible that the CI number should be even a bit higher if the next higher excitations ($7\,^1E$, $8\,^1E$, and $4\,^1B_2$) would also carry non-negligible oscillator strength in a more extensive CI study. For the total polarizability, we find 749 a.u. (LDA) and 853 a.u. (SAOP), of which the latter is consistent with the experimental values and our estimated CI result of 860. The test calculation with adapted bond lengths led to an increase of the SAOP polarizability of about 3%. For all sodium clusters studied here, the SAOP polarizabilities are larger than the LDA polarizabilities by roughly 10–15 %. As

TABLE VI. Na_8 absorption spectrum: comparison of LDA and SAOP results at BP-optimized D_{2d} geometry to experimental results and CI results at *ab initio* optimized D_{2d} geometry.

Label	Exc. En.[a]	Osc. Str.[b]	Exc. En.[a]	Osc. Str.[b]	Exc. En.[a]	Osc. Str.[b]	Exc. En.[a]	Intensity[c]
	CI [49][d]		LDA		SAOP		Expt. [62][e]	
$1\,^1E$	1.39	0.068	1.19	0.014	1.10	0.021		
$2\,^1E$	1.73	0.001	1.56	0.002	1.44	0.005		
$3\,^1E$	1.81	0.040	1.70	0.040	1.58	0.047		
$4\,^1E$	1.82	0.164	1.77	0.075	1.66	0.066		
$5\,^1E$	2.34	0.148	2.34	0.075	2.16	0.057	2.38	broad, weak
$6\,^1E$	2.53	3.200	2.60	0.852	2.42	0.671	2.53	strong
$7\,^1E$			2.66	0.424	2.49	0.629		
$8\,^1E$			2.71	1.718	2.55	1.620		
$9\,^1E$			2.78	0.034	2.63	0.033		
$10\,^1E$			2.86	0.239	2.67	0.595		
$\Sigma_i f_i(E)$[f]		3.62		3.47		3.74		
$1\,^1B_2$	1.65	0.002	1.49	0.003	1.38	0.001	1.68	broad, weak
$2\,^1B_2$	2.09	0.300	2.07	0.175	1.90	0.180	2.07	broad, weak
$3\,^1B_2$	2.51	2.040	2.46	0.760	2.29	0.715		
$4\,^1B_2$			2.62	1.155	2.46	1.202		
$\Sigma_i f_i(B_2)$[g]		2.34		2.09		2.10		
$-\varepsilon^{\mathrm{HOMO}}$[h]				3.04		4.60		
$\Sigma_i f_i$(total)[i]		5.96		5.57		5.84		
Contr. α[j]		753.4		629.9		749.7		
Other c. α[k]		(110)		118.9		103.2		
Total α[l]		(860)		748.8		852.9		

[a]Vertical excitation energies in eV.
[b]Oscillator strengths in a.u.
[c]General experimental description of the intensity of the bands.
[d]CI calculations from Ref. [48].
[e]Experimental results from Ref. [50].
[f]Sum of the oscillator strengths for the listed excitations of E symmetry.
[g]Sum of the oscillator strengths for the listed excitations of B_2 symmetry.
[h]Minus the orbital energy of the highest occupied KS orbital (in eV).
[i]Sum of all listed oscillator strengths of both E and of B_2 symmetry.
[j]The cumulative contribution of all listed excitations to the average polarizability.
[k]Contributions to the average polarizability coming from all higher-lying excitations which are not tabulated here. The CI number is estimated from the LDA and SAOP results.
[l]The total average polarizability (sum of the numbers listed under j and k). The CI number is based on the estimate under k.

far as the sodium clusters are concerned, the SAOP results are also consistently in better agreement with the experimental values (although a direct comparison without accounting for temperature effects should be considered as qualitative). It is also closer to the values estimated from the CI results than the LDA values are.

2. Li_8

The results for the Li_8 molecules are gathered in Table V. Here we again use an optimized structure of D_{2d} symmetry as this allows us to make straightforward comparisons to the Na_8 results and to CI results obtained in this symmetry. We do not claim that this is the most realistic structure. In fact, a BP-optimized ''centered trigonal prism'' (CTP) structure [47,56] is slightly lower in energy in DFT calculations, and we shall briefly comment below on some results in that geometry. However, and with the purpose of comparing various methods, the D_{2d} symmetry will be adopted.

There is one main experimental band in the Li_8 absorption spectrum, which is located in an energy region from about 2.3 to about 2.7 eV. In other words, it is rather broad, apart from being intense. Next to the CI results from the literature [53], we report our LDA and SAOP results. Similarly to Na_8, the oscillator strength is more fragmented in the TD-DFT results than in the CI results. The most intense theoretical peaks are positioned in the energy region 2.55–2.75 eV (with most of the oscillator strength at the higher energy) and are therefore somewhat higher than the experimental band centered around about 2.5 eV. Remarkably, and unlike the case for Li_4, the LDA excitation energies are consistently very close to the SAOP results (the largest deviation is equal

to only 0.05 eV). Looking at the oscillator strengths, we note that the summed CI oscillator strengths (4.6) are close to the sum for the SAOP potential (4.7), while the LDA result is about 10% lower (4.2).

If we calculate the contributions to the average polarizability coming from the tabulated transitions, we find the CI (partial) polarizability to be the largest with 581.6 a.u., followed by the SAOP result of 563.8 a.u. and finally the LDA result of 493.0 a.u. The large difference between the SAOP and LDA values is related to the oscillator strengths in this case, not to the excitation energies. In turn, the larger SAOP oscillator strength can be related to the larger values for the transition dipole moments between occupied and virtual KS orbitals. As expected, the small contribution of high-lying excitation energies to the polarizabilities is overestimated by the LDA potential, in comparison to the SAOP potential. Again this can be attributed to the incorrect shape of the LDA potential, as for the prototype molecules N_2, CO, etc. In the used basis set, the value for $-\varepsilon^{\mathrm{HOMO}}$ is 3.04 eV for the LDA potential and 4.60 for the SAOP potential, which means that the LDA excitation energies are still at a safe distance from this critical number.

As regards the total polarizabilities, we can compare to an experimental value of 560 a.u., with a significant error margin of about 10%. As such, the LDA result is in best agreement with experiment. The SAOP result is too high, and, if we add an estimate for the contribution of the higher excitations of 70 or 80 a.u., the CI number is also considerably too high. On the basis of theoretical overestimations for the peak positions, one would instead expect an underestimation of the experimental value. It is also surprising that the approach which should *a priori* be classified as the lowest level one, the LDA, gives the best agreement with experiment.

There are several possibilities to explain this. First, the used geometries are not close enough to the actual experimental geometry, which could lead to artificially good agreement between the LDA and experimental polarizabilities. In fact, some test calculations in the probably more realistic BP-optimized CTP structure reveal that the DFT polarizabilities are about 5% smaller in that geometry than in the D_{2d} geometry considered here. That would improve the agreement with experimental values.

However, temperature effects can be expected to have effects similar to those found for Na clusters in Ref. [10], which means that all $T=0$ theoretical polarizability values should be lower than the higher temperature experimental polarizability. Clearly, further investigations will be needed to connect reliable polarizability and absorption spectra results for Li_8.

IV. SUMMARY AND FUTURE PROSPECTS

Using recently developed xc potentials, which include features that are present in the exact xc potential but missing in the LDA xc potential, such as the correct $-1/r$ asymptotic behavior (LBα, SAOP), and the intershell peaks in the inner region (SAOP), we have shown that there is a considerable influence of the choice of xc potential on the calculated polarizability and absorption spectra results of small alkali-metal clusters. Because of the high-quality results obtained earlier for a small set of prototype molecules, the SAOP results are of special interest. The differences in the polarizability results have been connected to the differences found for the low-lying excitation energies and oscillator strengths. It has been shown that both the LDA and the SAOP results are in good agreement with both experimental and CI results, both for the absorption spectra and the polarizabilities.

Typically, the LDA potential leads to small overestimations for polarizabilities of small molecules of nonmetallic elements, because its xc potential is not attractive enough (leading to valence electrons which are too loosely bound), due to its shape in the (outer) valence region. Our results indeed seem to suggest that this problem is still present for the higher-lying LDA excitations, but for the alkali-metal clusters this effect is less important than the inner region of the xc potential. Indeed, the average polarizabilities are mostly determined by contributions from the low-lying excitation energies (as gathered in our tables), which are in turn determined by the xc potential in the inner region of the molecule. For this reason no significant improvements are to be expected from xc potentials which merely improve the outer region.

As far as uncertainties related to temperature effects and geometries are concerned, the clearest conclusions can be drawn for the smallest clusters. For the dimers Li_2, Na_2, and K_2, the SAOP polarizabilities and excitation energies at the experimental geometries are closer to the experimental values than the LDA results are, which provides further support for the ideas behind the modeling of this new xc potential. The LDA results for the dimers most clearly display the breakdown of this approximation for the high-lying excitations, which is also present in larger clusters, although the results for the important low-lying excitations are in fact rather good.

For the absorption spectra of the tetramers both the LDA and SAOP results are overall in excellent agreement with the experimental peaks and the CI assignments from the literature. The peak positions from the LDA and SAOP calculations for Li_4 and Na_4 deviate less than 0.1 eV on average from the experimental results, which is to be considered very satisfactory. The SAOP excitation energies are systematically lower than the LDA results. The SAOP polarizability for Li_4 is clearly larger than the experimental, CI, and LDA results. This is related to the slightly lower excitation energies and slightly larger oscillator strengths found with the SAOP potential. All theoretical polarizability results are larger than the experimental value. For Na_4 the SAOP polarizability is larger than the LDA polarizability and in much better agreement with experimental and CI results. The experimental G and H bands cannot be reliably assigned by the LDA because the underlying finite-basis expansion does not allow for such assignments in this relatively high energy region.

For the octamers the uncertainties are largest. Although the LDA and SAOP results for the absorption spectra are again in good agreement with the experimental peak positions, at least for the single dominating broad peak, some notable differences occur with respect to the CI assignments.

In the DFT results there are more excitations in the same energy range, and for the main band there are several excitations which come into play instead of a single excitation in the CI results. We checked for Na_8 that it is improbable that these differences can be attributed entirely to geometric differences. DFT results suggest that more structure should be present than the single broadband in the currently available experiments, a feature which may disappear if experiments are carried out at low temperatures. The Na_8 and Li_8 SAOP polarizabilities are again larger than their LDA counterparts. For Na_8 this improves agreement with the reference values. For Li_8 the SAOP result is overestimated with respect to experiment, but in better agreement with the CI value. The use of a CTP structure for Li_8 would have led to about 5% smaller DFT polarizabilities, in better agreement with experiment. Although there are uncertainties with respect to the choice of geometry and the influence of temperature effects, we can state that both the LDA and SAOP results provide a reliable basis for further studies on alkali metal clusters.

Several follow-up studies can be undertaken. It is certainly within computational limits to treat much larger neutral and charged clusters within the TDDFT framework. Also clusters with Cu, Ag, and Au atoms can be treated for which relativistic effects can be taken into account using the ZORA approach [57] implemented in ADF. The main limitation in the accuracy of such applications may turn out to be the determination of a reliable molecular geometry.

ACKNOWLEDGMENTS

We thank Igor Vasiliev and James Chelikowsky (University of Minnesota) for sharing some of their sodium cluster results with us, and for useful discussions on the differences between all-electron and pseudopotential calculations on absorption spectra. J.M.P. would like to acknowledge financial support from the Ministry of Science and Technology under Contract No. PRAXIS/C/FIS/10019/98.

[1] *Metal Clusters, Wiley Series in Theoretical Chemistry*, edited by Walter P. Ekardt (Wiley, New York, 1999), Vol. X.
[2] S. Kümmel, M. Brack, and P.-G. Reinhard, Phys. Rev. B **58**, R1774 (1998).
[3] S. Kümmel, T. Berkus, P.-G. Reinhard, and M. Brack, Eur. Phys. J. D **11**, 239 (2000).
[4] P. Calaminici, K. Jug, and A. M. Köster, J. Chem. Phys. **111**, 4613 (1999).
[5] I. Vasiliev, S. Öğüt, and J. R. Chelikowsky, Phys. Rev. Lett. **82**, 1919 (1999).
[6] I. Moullet, J. L. Martins, F. Reuse, and J. Buttet, Phys. Rev. Lett. **65**, 476 (1990).
[7] I. Moullet, J. L. Martins, F. Reuse, and J. Buttet, Phys. Rev. B **42**, 11 598 (1990).
[8] J. M. Pacheco and W.-D. Schöne, Phys. Rev. Lett. **79**, 4986 (1997).
[9] See the contribution of V. Bonačić-Koutecký *et al.* to *Metal Clusters* (Ref. [1]), and references therein.
[10] S. Kümmel, J. Akola, and M. Manninen, Phys. Rev. Lett. **84**, 3827 (2000).
[11] J. M. Pacheco and S. J. A. van Gisbergen (unpublished).
[12] U. Röthlisberger and W. Andreoni, J. Chem. Phys. **94**, 8129 (1991).
[13] José Luís Martins, J. Buttet, and R. Car, Phys. Rev. B **31**, 1804 (1985).
[14] K. Yabana and G. F. Bertsch, Phys. Rev. B **54**, 4484 (1996).
[15] S. J. A. van Gisbergen, J. G. Snijders, and E. J. Baerends, Comput. Phys. Commun. **118**, 119 (1999).
[16] M. Petersilka, U. J. Gossmann, and E. K. U. Gross, in *Electronic Density Functional Theory: Recent Progress and New Directions*, edited by J. F. Dobson, G. Vignale, and M. P. Das (Plenum, New York, 1998), pp. 177–197.
[17] S. J. A. van Gisbergen, F. Kootstra, P. R. T. Schipper, O. V. Gritsenko, J. G. Snijders, and E. J. Baerends, Phys. Rev. A **57**, 2556 (1998).
[18] P. R. T. Schipper, O. V. Gritsenko, S. J. A. van Gisbergen, and E. J. Baerends, J. Chem. Phys. **112**, 1344 (2000).
[19] K. Burke, M. Petersilka, and E. K. U. Gross, e-print cond-mat/0001153.
[20] R. van Leeuwen and E. J. Baerends, Phys. Rev. A **49**, 2421 (1994).
[21] O. V. Gritsenko, P. R. T. Schipper, and E. J. Baerends, Chem. Phys. Lett. **302**, 199 (1999).
[22] S. H. Vosko, L. Wilk, and M. Nusair, Can. J. Phys. **58**, 1200 (1980).
[23] S. A. C. McDowell, R. D. Amos, and N. C. Handy, Chem. Phys. Lett. **235**, 1 (1995).
[24] S. J. A. van Gisbergen, J. G. Snijders, and E. J. Baerends, J. Chem. Phys. **103**, 9347 (1995).
[25] S. J. A. van Gisbergen, V. P. Osinga, O. V. Gritsenko, R. van Leeuwen, J. G. Snijders, and E. J. Baerends, J. Chem. Phys. **105**, 3142 (1996).
[26] J. Guan, M. E. Casida, A. M. Köster, and D. R. Salahub, Phys. Rev. B **52**, 2184 (1995).
[27] W. Ekardt, Phys. Rev. Lett. **52**, 1925 (1984).
[28] W. Ekardt, Phys. Rev. B **31**, 6360 (1985).
[29] W. D. Knight, K. Clemenger, W. A. de Heer, and W. A. Saunders, Phys. Rev. B **31**, 2539 (1985).
[30] R. W. Molof, H. L. Schwartz, T. H. Miller, and B. Bederson, Phys. Rev. A **10**, 1131 (1974).
[31] O. V. Gritsenko, R. van Leeuwen, E. van Lenthe, and E. J. Baerends, Phys. Rev. A **51**, 1944 (1995).
[32] Oleg V. Gritsenko, Robert van Leeuwen, and Evert Jan Baerends, Int. J. Quantum Chem. **61**, 231 (1997).
[33] A. Rosa, G. Ricciardi, E. J. Baerends, and S. J. A. van Gisbergen, J. Phys. Chem. A (to be published).
[34] M. Grüning, O. V. Gritsenko, S. J. A. van Gisbergen, and E. J. Baerends, J. Chem. Phys. **114**, 652 (2001).
[35] A. D. Becke, Phys. Rev. A **38**, 3098 (1988).
[36] J. P. Perdew, Phys. Rev. B **33**, 8822 (1986).
[37] E. J. Baerends ADF 1999, A. Bérces, C. Bo, P. M. Boerrigter, L. Cavallo, L. Deng, R. M. Dickson, D. E. Ellis, L. Fan, T. H.

Fischer, C. Fonseca Guerra, S. J. A. van Gisbergen, J. A. Groeneveld, O. V. Gritsenko, F. E. Harris, P. van den Hoek, H. Jacobsen, G. van Kessel, F. Kootstra, E. van Lenthe, V. P. Osinga, P. H. T. Philipsen, D. Post, C. C. Pye, W. Ravenek, P. Ros, P. R. T. Schipper, G. Schreckenbach, J. G. Snijders, M. Sola, D. Swerhone, G. te Velde, P. Vernooijs, L. Versluis, O. Visser, E. van Wezenbeek, G. Wiesenekker, S. K. Wolff, T. K. Woo, and T. Ziegler.

[38] http://www.scm.com

[39] C. Fonseca Guerra, J. G. Snijders, G. te Velde, and E. J. Baerends, Theor. Chem. Acc. **99**, 391 (1998).

[40] G. te Velde, F. M. Bickelhaupt, E. J. Baerends, S. J. A. van Gisbergen, C. Fonseca Guerra, J. G. Snijders, and T. Ziegler, J. Comput. Chem. (to be published).

[41] M. E. Casida, in *Recent Advances in Density-Functional Methods*, edited by D. P. Chong (World Scientific, Singapore, 1995), p. 155.

[42] Ch. Jamorski, M. E. Casida, and D. R. Salahub, J. Chem. Phys. **104**, 5134 (1996).

[43] J. M. Pacheco and W. P. Ekardt, Ann. Phys. (Leipzig) **1**, 254 (1992).

[44] J. M. Pacheco and W. P. Ekardt, Z. Phys. D: At., Mol. Clusters **24**, 65 (1992).

[45] R. Antoine, D. Rayane, A. R. Allouche, M. Aubert-Frécon, E. Benichou, F. W. Dalby, Ph. Dugourd, and M. Broyer, J. Chem. Phys. **110**, 5568 (1999).

[46] M. E. Casida, C. Jamorski, K. C. Casida, and D. R. Salahub, J. Chem. Phys. **108**, 4439 (1998).

[47] http://tc.chem.vu.nl/~vgisberg/alkali.geo

[48] V. Bonačić-Koutecký, P. Fantucci, and J. Koutecký, Chem. Rev. **91**, 1035 (1991).

[49] V. Bonačić-Koutecký, P. Fantucci, and J. Koutecký, J. Chem. Phys. **93**, 3802 (1990).

[50] C. R. C. Wang, S. Pollack, D. Cameron, and M. M. Kappes, J. Chem. Phys. **93**, 3787 (1990).

[51] G. Onida, L. Reining, R. W. Godby, R. Del Sole, and W. Andreoni, Phys. Rev. Lett. **75**, 818 (1995).

[52] H. Haberland, in *Metal Clusters*, edited by W. Eckardt (Wiley, New York, 1999), pp. 181–210.

[53] J. Blanc, V. Bonačić-Koutecký, M. Broyer, J. Chevaleyre, Ph. Dugourd, J. Koutecký, C. Scheuch, J. P. Wolf, and L. Wöste, J. Chem. Phys. **96**, 1793 (1992).

[54] V. Bonačić-Koutecký, P. Fantucci, and J. Koutecký, Chem. Phys. Lett. **146**, 518 (1988).

[55] J. M. Pacheco and R. A. Broglia, Phys. Rev. Lett. **62**, 1400 (1989).

[56] J. M. Pacheco and J. L. Martins, J. Chem. Phys. **106**, 6039 (1997).

[57] E. van Lenthe, E. J. Baerends, and J. G. Snijders, J. Chem. Phys. **99**, 4597 (1993).

[58] V. Tarnovsky, M. Bunimovicz, L. Vušković, B. Stumpf, and B. Benderson, J. Chem. Phys. **98**, 3894 (1993).

[59] W. Müller and W. Meyer, J. Chem. Phys. **85**, 953 (1986).

[60] K. Clemenger, Ph.D. thesis, University of California at Berkeley, 1995.

[61] *Molecular Spectra and Molecular Structure, Volume I, Spectra of Diatomic Molecules*, 2nd ed., edited by G. Herzberg (Krieger, Malabar, FL, 1989).

[62] C. R. C. Wang, S. Pollack, and M. M. Kappes, Chem. Phys. Lett. **166**, 26 (1990).